Ion kinetic transport in TJ-II

J.L. Velasco[*,†], F. Castejón[**,*], L.A. Fernández[*,‡], V. Martin-Mayor[*,‡] and A. Tarancón[*,†]

[*]*BIFI: Instituto de Biocomputación y Física de Sistemas Complejos, 50009-Zaragoza, Spain*
[†]*Departamento de Física Teórica. Universidad de Zaragoza, 50009-Zaragoza, Spain*
[**]*Laboratorio Nacional de Fusión—Asociación Euratom/Ciemat, 28040-Madrid, Spain*
[‡]*Departamento de Física Teórica I. Universidad Complutense de Madrid, 28040-Madrid, Spain*

Abstract. The ion Drift Kinetic Equation (DKE) which describes the ion collisional transport is solved for the TJ-II device plasmas. This non-linear equation is computed by performing a *mean field* iterative calculation. In each step of the calculation, a Fokker-Planck equation is solved by means of the Langevin approach: one million particles are followed in a realistic TJ-II magnetic configuration, taking into account collisions and electric field. This allows to avoid the assumptions made in the usual neoclassical approach, namely considering radially narrow particle trajectories, diffusive transport, energy conservation and infinite parallel transport. As a consequence, global features of transport, not present in the customary neoclassical models, appear: non-diffusive transport and asymmetries on the magnetic surfaces.

Keywords: plasma kinetic equations, non-linearity, Langevin, Stellarator
PACS: 52.25.Dg, 52.65.-y, 52.65.Pp, 52.55.Hc

INTRODUCTION

The collisional transport in magnetic fusion devices, when properly taken into account, is a lower limit of the full transport that appears in these devices (the actual transport is given by the collisional plus the turbulent fluxes). The collisional fluxes are customarily estimated by using the standard neoclassical techniques. They consist of solving the Drift Kinetic Equation (DKE) under several hypothesis, the main of which are: 1) the radial excursion of particles in a single collision time must be smaller than the typical scale lengths of the magnitudes relevant for transport; 2) the parallel transport (along the magnetic field lines) is able to overcome the inhomogeneities that appear on every magnetic surface (this is equivalent to consider that the transport equations are only one-dimensional in real space); 3) the transport is diffusive, i. e., the fluxes can be written as transport coefficients times the thermodynamical forces, which are the gradients of the macroscopic plasma magnitudes; 4) the particle kinetic energy is conserved in the collision time scale; 5) the velocity distribution function is very close to the Maxwellian.

In the present work, we present a method to solve the DKE without the standard neoclassical assumptions, which allows us to explore effects that cannot be described or predicted using such approximations. ISDEP (Integrator of Stochastic Differential Equations in Plasmas), which is a non-linear full-f Monte Carlo code, has been developed and applied to the complex geometry of the TJ-II stellarator, a medium size flexible heliac ($R = 1.5$ m, $a < 0.22$ m) [1]. This device is characterized by the difficulty

CP1071, *Large Scale Simulations of Complex Systems, Condensed Matter and Fusion Plasma, BIFI 2008 International Conference*, edited by P. Bruscolini, J. Clemente-Gallardo, P. Echenique, J. F. Sáenz-Lorenzo, and F. Castejón,

of estimating the transport by using standard techniques [2]. Moreover, the assumptions on which those techniques are based are not fulfilled in the long mean free path regime of TJ-II plasmas. A way of overcoming these difficulties is to estimate the collisional transport by calculating complete ion trajectories in the guiding centre approximation, taking into account the electric field and the collisions with thermal electrons and ions. The definition of a fixed background plasma is also a customary approach in neoclassical models. Nevertheless, a background plasma acts as an infinite thermal bath, as will be discussed below, and affects the ion trajectories in a way that precludes the simulation of non-linear effects, such as plasma heating. In these cases, it is necessary to let the background plasma evolve, in a way consistent with the calculated trajectories.

Important transport consequences can be extracted from the properties of particle trajectories calculated with ISDEP: the particle radial excursions are shown to be wider than the characteristic lengths of the plasma in a single collision time, thus contradicting the local ansatz. As a consequence of this, the flux is shown to be non-diffusive. Non-negligible asymmetries can be observed as a consequence of this non-local transport. In particular, an inhomogeneous distribution of particles along the poloidal angles is observed on every magnetic surface.

Besides the estimates presented in this work, the study of ion trajectories in low collisionality plasmas is very important both for tokamaks and stellarators. Several issues make this study useful to understand the confinement in these devices: the behaviour of particles in a given magnetic configuration, the confinement of fast ions and alpha particles (see e.g. [3, 4]), the evaluation of direct losses, and the effect of magnetic ripple on particle confinement. This is also important in tokamaks [5, 6]: it has been recently claimed [7] that the ITER magnetic field will have a clearly three-dimensional structure, with important implications in alpha-particle confinement.

MOTIVATION

The violation of neoclassical assumptions

The customary neoclassical transport estimates consider that the fluxes can be written as the thermodynamical forces times the transport coefficients. The latter are estimated by solving the DKE under the hypothesis that they depend only on local plasma characteristics, namely the magnetic structure, the local electric field and the collisionality. It is also assumed that the kinetic energy of the particles is conserved. The first of these hypothesis is equivalent to the assumption that the typical size of the trajectories performed in a collision time is small; the second implies that the particles do not gain or lose energy during their trajectories in the absence of collisions.

However, due to the complexity of the TJ-II magnetic configuration and the presence of electrostatic potential, some ion orbits include large radial excursions and their kinetic energy changes substantially in a single collision time. Indeed, the typical excursions are wider than the characteristic gradient lengths of density, temperature and electrostatic

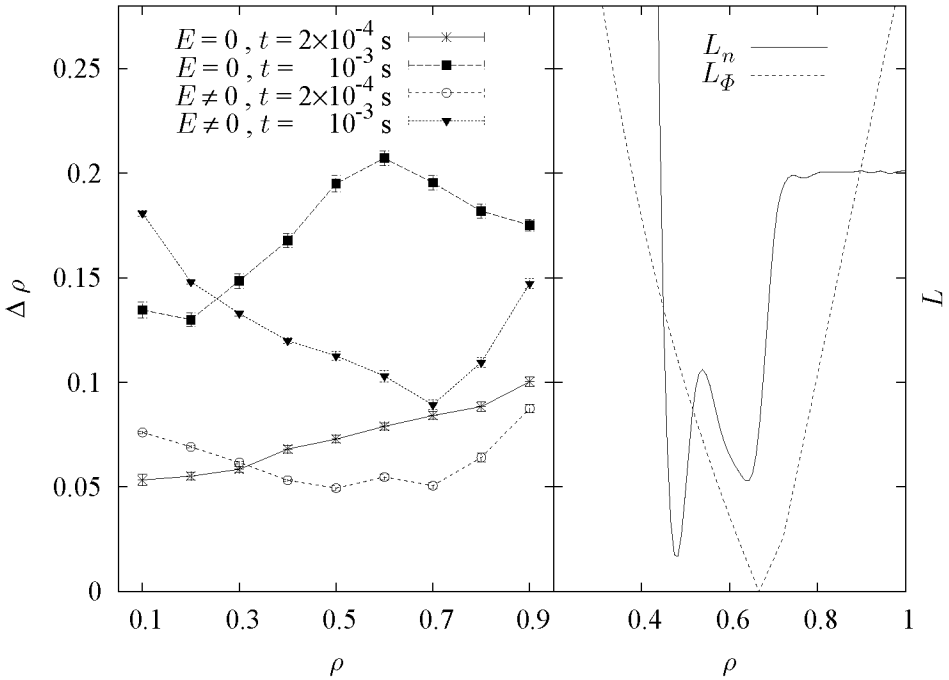

FIGURE 1. (Left) Orbit sizes, with and without electric field, for trajectories starting at several radial positions. The selected times, $t = 2 \times 10^{-4}$ s and $t = 10^{-3}$ s, are approximately the collision times in the centre and in the edge of the plasma respectively. (Right) Characteristic length-scales of the plasma obtained from the gradients of the density and the potential profiles.

potential, so that the ions visit plasma regions of widely differing conditions, which invalidates the local ansatz.

This was calculated in a previous work [8], where transport properties were estimated by launching a large number of ions and following their trajectories during approximately two collision times. Although collisions were not included, it could be concluded that, under the influence of realistic TJ-II magnetic and electric fields, the typical radial width of orbits in a single collision time is comparable with the relevant spacial scales of the plasma.

This assertion can be made more precise for a typical TJ-II ECRH (Electron Cyclotron Resonance Heating) plasma: we compare in Fig. 1 the typical size of the radial excursions with the relevant length scales of our plasma (which are calculated, included collisions, as shown in the following section). The profiles, corresponding to a typical ECRH plasma, are taken from [9], and are qualitatively similar to those shown in Fig. 2. The calculated orbit sizes are defined as:

$$\Delta\rho(t) \equiv \langle (\rho(t) - \rho(0))^2 \rangle^{1/2}, \qquad \rho \equiv \sqrt{\phi/\phi_0}. \tag{1}$$

Here, ρ is the normalized radial coordinate, while ϕ and ϕ_0 are the magnetic fluxes

through the local and the last closed magnetic surfaces. The trajectories start at several (uniformly distributed) radial radial positions with velocities distributed according to a Maxwellian. In a collision time, the calculated sizes reach 20% of the plasma minor radius in the case without field. In the presence of electric field, the width of the orbits is smaller: in the centre of the plasma lays between 5% and 10% of the minor radius for $t \sim 10^{-4}$ s, and between 10 and 15% for $t \sim 10^{-3}$ s. This is to be compared (see Fig. 1-right) with the characteristics lengths of the relevant magnitudes of the plasma: for the density, we have $L_n \equiv |n/\nabla\rho| \approx 0.2$ in a wide region (ρ between 0.4 and 0.7) of the plasma. The same happens with the electric potential, whose characteristic length is described by $L_\phi \equiv |(\phi - \phi_{min})/\nabla\phi|$. The quantity $L_B \equiv |B/\nabla B|$, although highly non-uniform, is of the order of the macroscopic size of the device. Therefore the orbits can be wider or of the order of the gradient lengths of density and electric potential in the zones of strongly varying density (ρ between 0.4 and 0.7) and electric potential (ρ between 0.4 and 0.8).
Very recently, other efforts have been done in order to include, for instance, finite-orbit-width in simulations in δf MC models devices [10] and in gyrokinetic codes [11]. The results in these calculations have stressed the importance of a non-local treatment of neoclassical transport.

Moreover, the potential profile in typical ECH plasmas (see Fig. 2) can vary several hundreds of volts from the centre to the edge. Therefore the change in potential energy is far from being negligible in comparison with the typical ion temperatures ($\sim 100\,\mathrm{eV}$).

Finally, the standard neoclassical transport assumes that all the relevant magnitudes are constant on every magnetic surface and, consequently, transport equations can be written in one dimension. Nevertheless, up-down asymmetries due mainly to the effect of the $\vec{E}\times\vec{B}$ drifts are observed experimentally [12], as well as toroidal asymmetries, due to the effect of trapped particles [9].

Non-linear phenomena

The DKE equation is usually solved by means of linearization, i.e. defining a background ion distribution. Then, the evolution of the distribution function of *test* ions in the presence of a fixed distribution of *field* ions is described by a Fokker-Planck equation. This is what we call a linear calculation, and it is a reasonable approach when the test ion distribution does not separate too much from that of the field ions. Nevertheless, it cannot be used as such to calculate a variety of non-linear phenomena, such as plasma heating, either by interaction with the waves or by confinement improvement: the background distribution acts as an infinite thermal bath retaining all the extra energy received by the test ions. The background ion distribution must be therefore modified, according to the variations in that of the test ions. This kind of computation, which we will call in the text non-linear calculation, can be also implemented for the Langevin approach of ISDEP.

An example of application of a full-f method is the study of the ion heating during the transitions to CERC (Core Electron Root Confinement) [13]. In stellarator devices, transitions to improved core electron-root confinement (CERC) are established in conditions of high Electron Cyclotron Heating (ECH) absorbed power density (see the review [14] and references therein). These regimes have been found in different helical devices: the Compact Helical System [15], Wendelstein 7-AS [16], the Large Helical Device [17] and TJ-II [18] (in the latter, provoked by the introduction of a rational value of rotational transform [19]). These transitions are characterized by the appearance of a peaked electron temperature profile and a large positive electric field in the core plasma region. The electron temperature increase in the core plasma, caused by ECH heating, enhances the outward electron flux. The ambipolar condition is then fulfilled by the existence of a positive electric field, which reduces the $\vec{\nabla}B$ drift of the ripple-trapped electrons [14].

The relevant phenomena observed in TJ-II, that makes mandatory to use a non-linear calculation, is the increase of the ion temperature (about a 10 — 15%) observed during the transition [19], synchronized with that of the electron temperature. In a previous work [13], it is checked that only two ingredients, electron-ion energy exchange and enhanced confinement by the electric field are enough to reproduce the experimental findings. The electric field also contribute to the ion heating by communicating energy to the ions that drift outwards.

The delay between the change in the ion temperature and that of the electron temperature is about 2 — 3 ms, of the order of the time scale that the ions take to react to changes in the electric field [9]. The electron-ion collision time is 10^{-2} s — 10^{-1} s. Since both characteristic times are much longer than the ion-ion collision time (10^{-4} — 10^{-3} s), a linear Fokker-Planck calculation cannot properly reproduce any ion temperature increase caused by the electrons or the electric field.

In [13], the ion heating in the transition to CERC is estimated, by solving the DKE equation in the plasma conditions before and after the transitions. The results show quantitative agreement with the experiment, and support the hypothesis of ion heating via electron-ion transfer and enhanced ion confinement in our plasma conditions.

THE ISDEP CODE

Following the well-known guiding-centre approximation (see e.g. [20]), our five-dimensional space consists of the position of the guiding center of the Larmor precession, $\vec{r}_{\mathrm{GC}}$, the pitch λ and the normalized particle kinetic energy x^2:

$$x^2 \equiv \frac{v^2}{{v_{\mathrm{th}_i}}^2} \quad , \quad v_{\mathrm{th}_i} = \sqrt{\frac{2kT_i}{m_i}} \quad , \quad \lambda \equiv \frac{v_{\|}}{\sqrt{v^2}}, \tag{2}$$

where m_i is the mass of the ions, T_i the ion temperature and k the Boltzmann constant.

The problem addressed here is to solve for the evolution of the five dimensional full distribution function $f(t,\vec{r}_{\rm GC},\lambda,x^2)$ of the ions in the plasma. Under several non-restrictive hypothesis (guiding-center approximation, long range collisions), it can be modeled with a Fokker-Planck-like equation:

$$\frac{\partial f}{\partial t}+\vec{\nabla}_{r_{\rm GC}}\cdot(\vec{a}_{r_{\rm GC}}f)+\frac{\partial}{\partial\lambda}(a_\lambda f)+\frac{\partial}{\partial x^2}(a_{x^2}f)=\mathscr{L}f. \tag{3}$$

This is a highly non-linear equation, since the coefficients $a_{r_{\rm GC}}$, a_λ, a_{x^2} and $\mathscr{L}$ do depend on the ion distribution function f. The collision operator includes collisions with electrons and ions. It is and extended form of that of Boozer and Kuo-Petravic [22] developed following [21]. The former is based on previous results by Rosenbluth *et al.* [23]. The basic assumption is that each collision involves only two particles and produces mainly small angle scattering. The rest of coefficients follow from the usual guiding center approximation. Their explicit form is shown in [9] and [13].

Our approach to this non-linear problem is to undertake a mean field calculation of the non-linear (NL) equation. At each iteration of the mean field calculation, the NL equation is linearized, thus becoming a Fokker-Planck (FP) equation, and solved. The solution is then used to construct a new FP for the next iteration.

Linearization is accomplished by splitting the distribution function in two terms, describing separately field and test ions:

$$f=f^{\rm field}+f^{\rm test} \tag{4}$$

The only assumption made on the shape of $f^{\rm test}$ is that it equals $f^{\rm field}$ at the initial instant $t=0\,{\rm s}$. It is also assumed that the ions represented by $f^{\rm test}$ have little weight on the full ion distribution f. As a consequence of this, their behaviour does not affect the value of $a_{r_{\rm GC}}$, a_λ, a_{x^2} and $\mathscr{L}$, which are only determined by $f^{\rm field}$. Therefore, once $f^{\rm field}$ is defined, this procedure yields the following FP equation for $f^{\rm test}$:

$$\frac{\partial f^{\rm test}}{\partial t}+\vec{\nabla}_{r_{\rm GC}}\cdot(\vec{a}_{r_{\rm GC}}f^{\rm test})+\frac{\partial}{\partial\lambda}(a_\lambda f^{\rm test})+\frac{\partial}{\partial x^2}(a_{x^2}f^{\rm test})=\mathscr{L}f^{\rm test}. \tag{5}$$

Let us now make a more detailed sketch of how the mean field calculation is accomplished: we define a field ion distribution $f_0^{\rm field}$, which is taken from the experiment (see below). This definition allows us to construct a FP equation for $f_0^{\rm test}$, with the initial condition $f_0^{\rm test}(t=0\,{\rm s})=f_0^{\rm field}(t=0\,{\rm s})$. The solution of this equation, which yields $f_0^{\rm test}$ for all t, is the point where usual calculations stop. On the contrary, in our full-f calculation, we use this solution to define a new field ion distribution $f_1^{\rm field}\equiv f_0^{\rm test}$ and construct a new FP equation. This scheme is iterated until we find a stationary solution, in which the test ion distribution function evolves "in equilibrium" with that of the thermal bath (i.e. $f_N^{\rm test}=f_N^{\rm field}\equiv f_{N-1}^{\rm test}$ when $N\to\infty$), under the influence of the external sources (namely the electric field and the background electrons).

Several points from the former scheme must be detailed. First of all, the field ion distribution is chosen to be, at each iteration, of the form:

$$f^{\text{field}}(t,\vec{r}_{\text{GC}},\lambda,x^2)=n(\vec{r}_{\text{GC}})\frac{x\,\mathrm{e}^{-x^2}}{\sqrt{\pi}}\,, \tag{6}$$

where $n(\vec{r}_{\text{GC}})$ is the number density of the physical ions. Therefore, our field plasma profiles depend only on the radial coordinate, and the momentum distributions are Maxwellian. The latter assumption is required by the collision operator. The former is taken for computational reasons: a three-dimensional precise measurement of the ion density and temperature is out of reach for this NL calculation. Nevertheless, although non exact, both simplifications are reasonable: non-zero but small asymmetries and non-Maxwellianities were measured in [9]. Therefore, in our scheme, $f_N^{\text{field}} \equiv f_{N-1}^{\text{test}}$ means that we measure the radial density and average kinetic energy profiles of the plasma from the function f_{N-1}^{test} and construct, following Eq. (6), the field distribution f_N^{field}. This is a fully self-consistent calculation of the full ion distribution function as long as the corrections to Maxwellianity and to the averages on magnetic surfaces are negligible. This will be further discussed below.

The second point regards the way that the linearized FP equation is solved. In a previous work (see [9] and references therein), a previous version of ISDEP was developed, which solves the guiding-centre equations of test ions in the presence of collisions with background ions. The ion dynamics are represented by a closed set of five coupled (Itô) stochastic differential equations (SDE):

$$\frac{\mathrm{d}\vec{r}_{\text{GC}}}{\mathrm{d}t} = \vec{a}_{r_{\text{GC}}}\,, \tag{7}$$

$$\frac{\mathrm{d}\lambda}{\mathrm{d}t} = \left[a_\lambda + a_\lambda^{\text{Ito}}\right] + b_\lambda \xi_\lambda\,, \tag{8}$$

$$\frac{\mathrm{d}x^2}{\mathrm{d}t} = \left[a_{x^2} + a_{x^2}^{\text{Ito}}\right] + b_{x^2} \xi_{x^2}\,, \tag{9}$$

where ξ_λ and ξ_{x^2} are independent white noises. Itô calculus guarantees that if the starting positions and velocities of the test ions are chosen according to $f_N^{\text{test}}(t=0\,\text{s})$, then their positions and velocities at an arbitrary time will be distributed according to the solution of the N-th FP equation, f_N^{test}. Therefore, in each step N of our procedure, a great number of test ion trajectories are calculated until $t=0.1\,\text{s}$. From the measurements over this ensemble, we obtain the test ion distribution f_N^{test}.
More concretely, the ion temperature and density are calculated at several radial coronas (10, according to the smoothness of the profiles) at several times (17, logarithmically distributed, a natural choice according to the time evolution of the system, note the logarithmic scale of Fig. 4). In the next iteration, the temperature at any time and radial position will be obtained by linear interpolation of these values.
The scheme is considered to have converged (i.e. $f_N^{\text{field}} \equiv f_{N-1}^{\text{test}}$) when the density and temperature profiles are independent of N within the error bars. Since our test distribution functions (and therefore our field distribution functions) can be time-dependent,

convergence must be checked for all times.

The collision operator $\mathscr{L}$ includes also collisions with background electrons, as discussed in [13]. These electrons also determine, via the ambipolarity condition, the electrostatic potential. Therefore, a self-consistent estimation of the electrostatic potential and the electron distribution function is to be included in future versions of the code. For the time being, we consider the electrons to be distributed according to a local Maxwellian and consider fixed the electric field, see Fig. 2.

The calculated density profiles are expected to be more hollow than the experimental ones (see Fig. 3) as a consequence of the lack of sources in the simulation. Therefore, for this low ion temperature plasma, the radial electric field represents a strong thermodynamic force that must be counteracted by such a hollow density profile.

For the integration of long trajectories in the complex TJ-II magnetic configuration, we use the algorithm developed by Kloeden and Pearson [24]. It is of the second order convergence in the deterministic part and of the first order of weak convergence in the presence of multiplicative Gaussian noises. For this algorithm to be employed, the former SDEs, which are of Itô type, must be written in their Stratonovich version (see [9] for details). A careful control of the errors induced by the time and space (see below) discretization, has been accomplished, as in the appendix of [9].

RESULTS OF LARGE SCALE RUNS

Non-linear effects

This calculation has been carried for a plasma representing the situation after the transition to CERC. We show its experimentally measured profiles in Fig. 2: it is characterized by a peaked electron temperature profile and a high positive electric field in the core region. The potential profile, taken similar to those obtained by HIBP measurements, presents a minimum around $\rho = 0.6$. The initial ion temperature profile, taken from CX measurements, is almost flat and the distribution function is a Maxwellian with temperature $T_i = 100\,\mathrm{eV}$. The density profiles are hollow. The actual 3D magnetic configuration is considered by using a grid fitted to the magnetic surfaces in the real space [25].

In Fig. 3, we show the convergence of the plasma profiles. We have simulated about 10^5 orbits in each iteration, in order to keep the errors in the profiles above 5%, so that numerical inaccuracy does not hide the evolution of the profiles with N. We find the final solution for the ion distribution after $N = 30$ iterations. This is the number of steps for the temperature profile to converge at the longer time needed, $t = 10^{-2}\,\mathrm{s}$, which is the toughest case; shorter times and the density profiles converge much faster. The latter is essentially governed by the electric field, which is fixed during the simulation, and therefore the non-linear effects are much less important.
At time $t = 10^{-2}\,\mathrm{s}$, the temperature in the core region has increased about 15%. It is

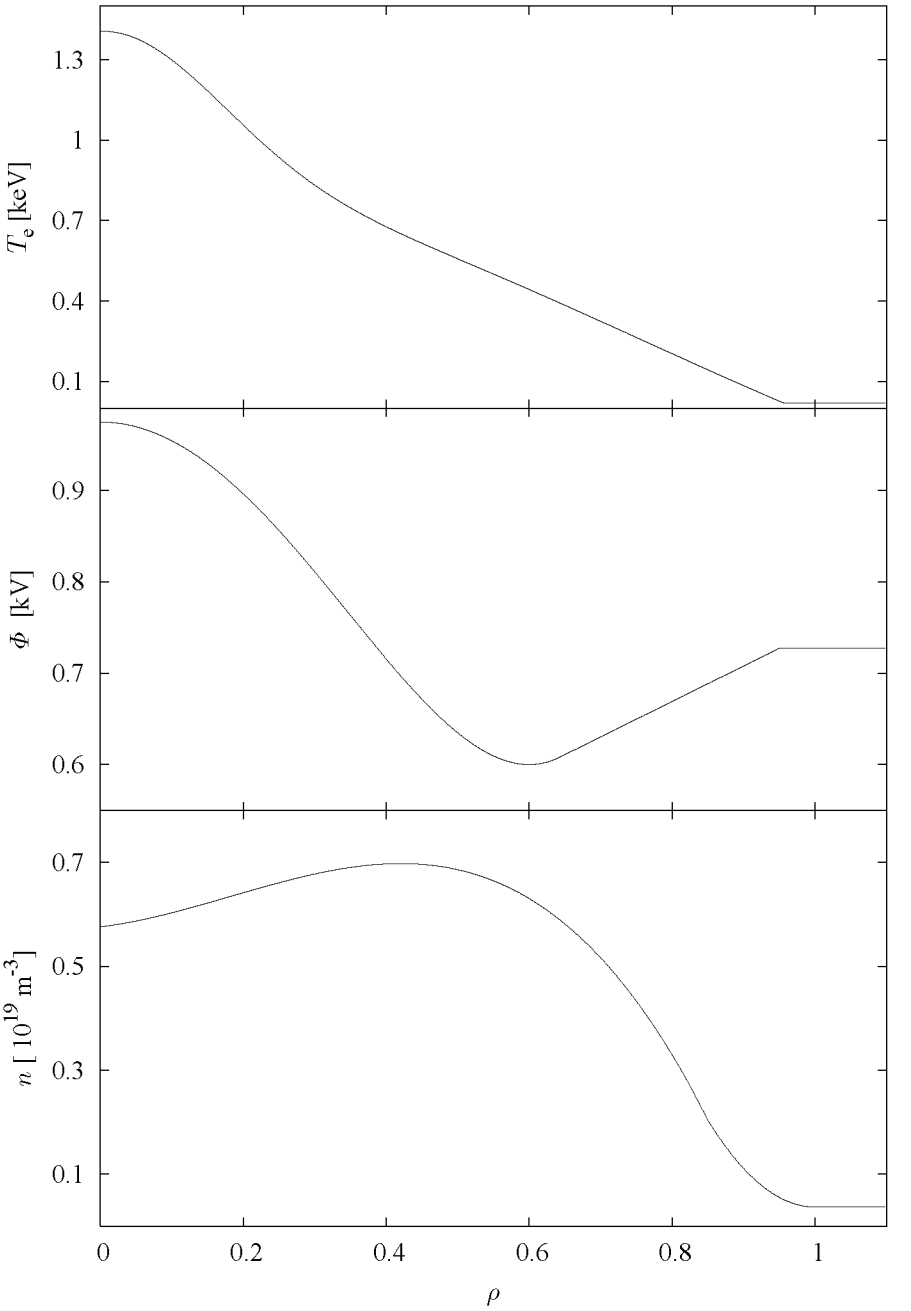

FIGURE 2. Plasma profiles: electron temperature, electrostatic potential and density as function of the radial coordinate.

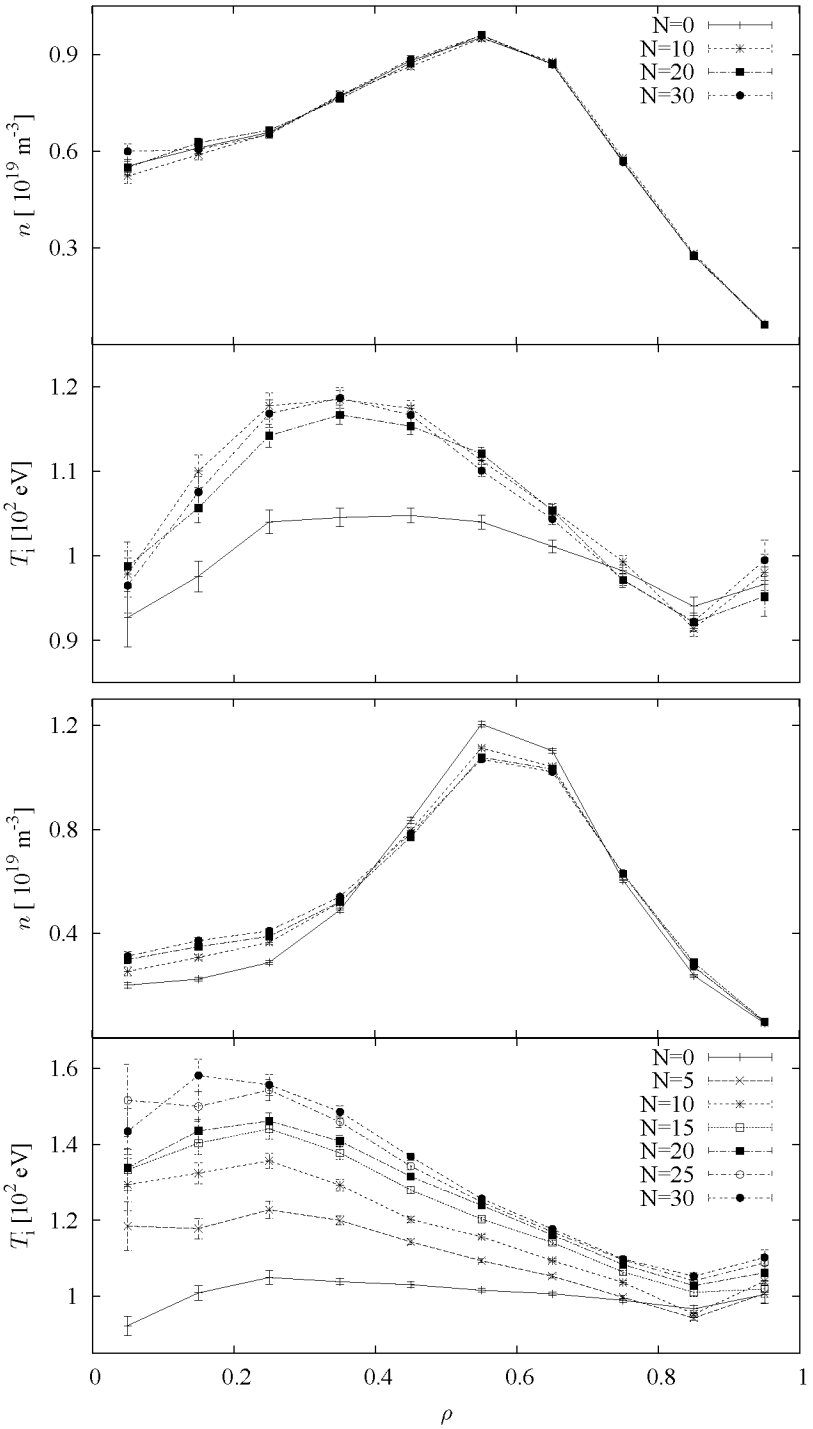

FIGURE 3. Radial profiles at $t = 10^{-3}$ s (up) and $t = 10^{-2}$ s (down) for several iterations N of the scheme.

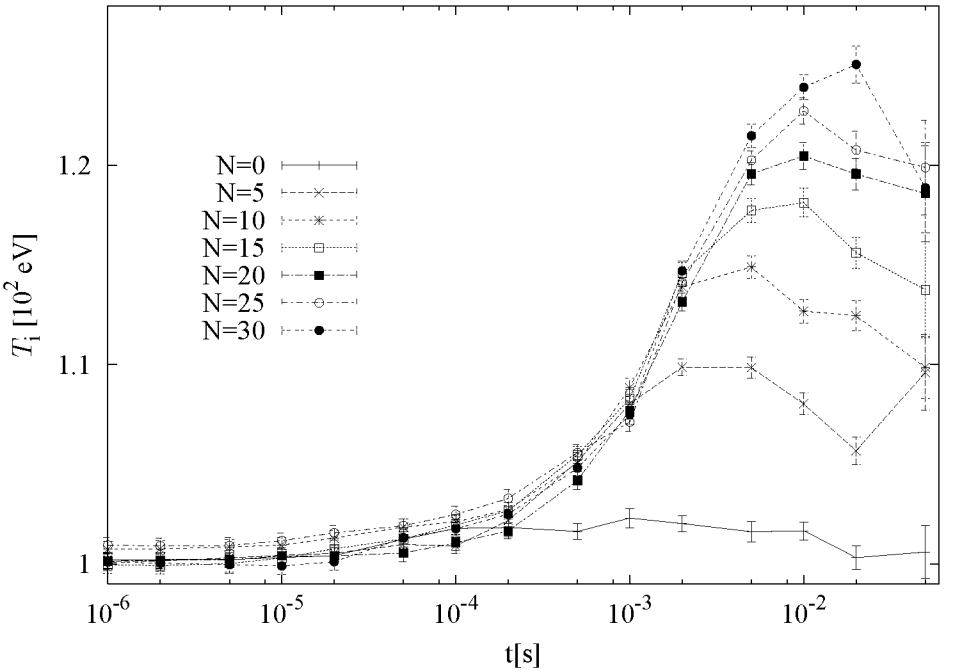

FIGURE 4. Average temperature of the ions as a function of time.

clear from Fig. 3 that ion heating could not be simulated by means of the linearized approach ($N = 0$ in our mean field calculation).

In Fig. 4, we show the time evolution of the average temperature of the ions. The final temperature is about 25% higher than the initial. It rises on a time scale of $t \sim 5 \times 10^{-3}$ s. In [9], it was shown that this is the characteristic time for the action of the electric field, which might be mainly responsible for this plasma heating.

Fig. 4 shows the adequacy of our full-f approach, since the linear approach has a major drawback: one imposes a time-independent ion temperature profile for the field particles. The ion-ion collision time (10^{-4} — 10^{-3} s) is lower than the other time scales relevant for the ion temperature, namely that of the ion-electron collision and that of the action of the electric field. In that time-scale, in $N = 0$, the field ions retain great part of the extra energy absorbed by the test ions from other sources, precluding the physical effect of electron-ion heating.

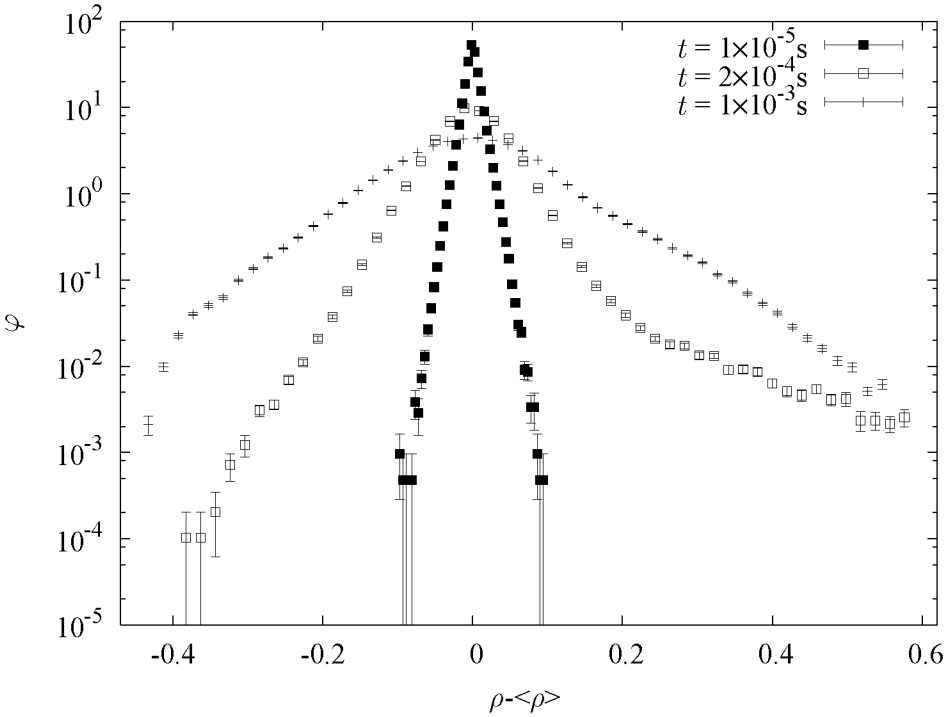

FIGURE 5. Probability density function (pdf) of the radial displacements of ions. The x-scale is shifted by $\langle\rho\rangle$. The collision time is $t \sim 2 \times 10^{-4}$s.

Non-diffusive transport

In Fig. 5 we show, for several selected times, the radial distribution of ions launched from a fixed radial position $\rho = 0.4$, and with a Maxwellian velocity distribution. Since $\langle\rho\rangle$ does not separate significantly from $\rho = 0.4$ for the times selected, this is equivalent to show to the probability density function (pdf) of the radial displacements of ions. For a time of the order of the collision time, a long tail has developed. Since ρ takes values between 0 and 1, Fig. 5 shows how, in a single collision time, there are particles that arrive to the edge of the plasma. The asymmetry in the pdf should be attributed to the asymmetry in the electrostatic potential well, see Fig. 2. At long times, the pdf is clearly non-Gaussian, as it would if transport were diffusive. Gaussianity of the pdf is the usual assumption for estimating neoclassical transport coefficients by Monte Carlo techniques.

We show in Fig. 6, the poloidal distribution of particles. We normalize it by the distribution at $t = 0$s. In that way, particles accumulate in regions where $\varphi > 1$. A slight asymmetry starts to develop at very short times and remains during all the simulated time. This time scale points at the magnetic structure as the origin of the asymmetry.
On the one hand, this effect is an asymmetry due to the complex magnetic configuration

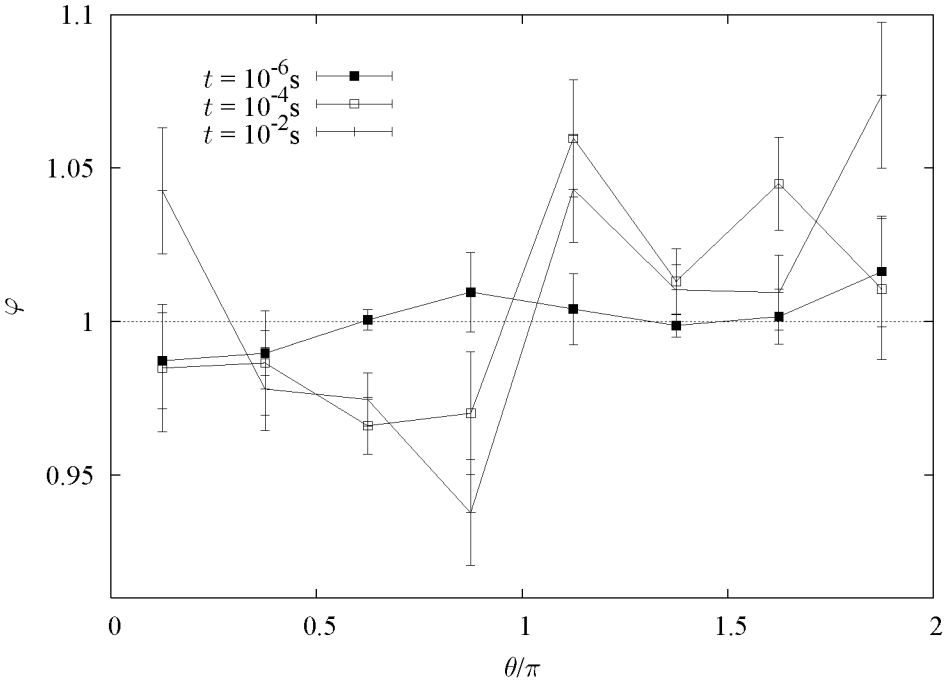

FIGURE 6. Poloidal distribution of particles at $t = 10^{-3}$ s for both plasmas. It must be 1 if the ions are uniformly distributed.

of TJ-II which cannot be calculated by the usual neoclassical calculations, which average on the magnetic surfaces. On the other hand, it is a measure of how self-consistent is our mean field method. Some points in the profiles are at two standard deviations from $\varphi = 1$. This is an estimate of how accurate is to construct our field distribution function by averaging on the magnetic surfaces the calculated test ion distribution function.
At first sight these two assertions may seem contradictory, but one may find a balance between them: the iterative scheme may be interpreted as a way of obtaining the FP equation that, under several simplifications (Maxwellianity and symmetry on the magnetic surfaces) better describes the physical system ($N \to \infty$). Then, the Langevin approach allows to solve it without these simplifications.

CONCLUSIONS

A full-f Montercarlo code has been developed and applied to the study of the collisional ion transport properties of the TJ-II plasmas. We have gone beyond the linear approximation used in a previous work [9] by introducing an iterative scheme more suited for the cases in which non-linear effects appear, such as plasma heating. The present approach is equivalent to performing a quasi-linear calculation, in the sense that

the background distribution function is a slowly varying function of a fast changing test distribution function, and the background electrostatic potential is unchanged. More precisely, the ion radial density and temperature profiles are calculated in a self consistent way. In the limit where the distribution function remains Maxwellian and there are not relevant asymmetries on the magnetic surfaces, this is a fully self-consistent calculation of the ion distribution function. The reason is that our collision operator is valid for Maxwellian distribution functions and, for computational reasons, the background distribution function after every iteration is obtained by averaging the ion distribution at every magnetic surface.

The novelty of these calculations is that they allow us to avoid the approximations that are used in the standard neoclassical theory, thus having a much better estimation of the ion collisional transport. Differently to the neoclassical theory no assumptions are made on the diffusive nature of transport. This allows us to estimate the exact fluxes and the plasma evolution, and actually to show that these fluxes are not diffusive in the TJ-II plasmas regime. Moreover, the estimation of the propagator in the effective radius ρ, shows clear non-Gaussian features in contradiction with the standard neoclassical calculations based on Monte Carlo methods. Our method considers the global rather than the local plasma properties on the particle trajectories properties, allowing us to perform estimations without the limitation of considering only small radial excursions in a collision time. The effect of these large excursion has been observed experimentally as an almost flat ion temperature profile [26]

No average on the magnetic surfaces is considered, differently to the standard neoclassical codes, which assume that the parallel transport is large enough to avoid any inhomogeneity on the magnetic surface. This fact permits us to obtain poloidal asymmetries due mainly to the effect of the complex magnetic structure of TJ-II.

ACKNOWLEDGMENTS

We acknowledge partial financial support from MEC (Spain), through research contract FIS2006-08533-C03, European Commission through contracts EGEE-II-031688 and int.eu.grid 031857, and from BSCH-UCM. J.L. Velasco is a DGA (Aragón, Spain) fellow. Great accuracy has been achieved thanks to the use of the computing platform Zivis [27].

REFERENCES

1. C Alejaldre *et al.*, *Fusion Technology* **17**, 131 (1990).
2. V Tribaldos and J Guasp, *Plasma Phys. Control. Fusion* **47**, 545 (2005).
3. W Lotz, P Merkel, J Nürenberg and E Strumberger, *Plasma Physics and Controlled Fusion* **34**, 1037 (1992).
4. S G Shasharina and J R Cary,*Nuclear Fusion* **33**, 648 (1993)
5. T Kurki-Suonio *et al.*, *Nucl. Fusion* **42**, 725 (2002)

6. T Kiviniemi *et al.*, "Ripple-induced fast ion and thermal ion losses," *32nd 2nd EPS Plasma Phys. Conference*, Tarragona, Spain 2005.
7. T Koskela *et al.*, "Alpha particle orbits in a locally perturbed ITER 3D magnetic field," in *35th EPS Plasma Phys. Conference*, Crete, Greece, 2008.
8. F Castejón *et al.*, *Fusion Science and Technology* **50**, 412 (2006).
9. F Castejón *et al.*, *Plasma Phys. Control. Fusion* **49**, 753 (2007).
10. S Satake *et al.*, *Nucl. Fusion* **45**, 1362 (2005).
11. W X Wang *et al.*, *Comp. Phys. Commun.* **164**, 178 (2004).
12. M A Ochando and F Medina, *Fusion Sci. Technol* **50** 313 (2006).
13. J L Velasco *et al.*, *Nucl. Fusion* **48**, 065008 (2008).
14. M Yokoyama *et al.*, *Fusion Sci. Technol.* **50**, 327 (2006).
15. A Fujisawa *et al.*, *Phys. Rev. Lett.*, **82** 2669 (1999).
16. H Maassberg *et al.*, *Phys. Plasmas* **7**, 295 (2000).
17. K Ida *et al.*, *Phys. Rev. Lett.* **86**, 5297 (2001).
18. F Castejón *et al.*, *Nucl. Fusion* **42**, 271 (2002).
19. T Estrada *et al.*, *Nucl. Fusion* **47**, 305 (2007).
20. R J Goldston and P H Rutherford, *Introduction to Plasma Physics*, IOP Publishing, Bristol, 1995.
21. T S Chen, *A General Form of the Coulomb Scattering Operators for Monte Carlo Simulations and a Note on the Guiding Center Equations in Different Magnetic Coordinate Conventions*, Max-Planck-Institut für Plasmaphysik IPP 0/50, Garching, 1988.
22. A Boozer and G Kuo-Petravic, *Plasma Physics* **24**, 851 (1981).
23. M N Rosenbluth, W MacDonald and D Judd, *Phys. Rev.* **107** 1 (1957).
24. P E Kloeden and R A Pearson, *The numerical solution of stochastic differential equations, J. Austral. Math. Soc., Ser* **B20**, pp. 8-12, 1977.
25. J Guasp and M Liniers, *Nuclear Fusion* **40**, 397 (2000).
26. J M Fontdecaba *et al.*, *Fusion Sci. Technol.* **46**, 271 (2004).
27. B. Antolí *et al.* "ZIVIS: A City Computing Platform Based on Volunteer Computing" Spanish Conference on E-Science Grid Computing Proceedings, Madrid, 2007, pp. 153.